

## Experimental Evidence of Dislocation Related Shallow States in *p*-Type Si

A. Castaldini,<sup>1</sup> D. Cavalcoli,<sup>1</sup> A. Cavallini,<sup>1</sup> and S. Pizzini<sup>2</sup>

<sup>1</sup>*Physics Department, University of Bologna, viale C. Berti Pichat 6/II I-40127 Bologna, Italy*

<sup>2</sup>*Materials Science Department, University of Milano-Bicocca, via Cozzi 53 I-20126 Milano, Italy*

(Received 13 December 2004; published 11 August 2005)

Theory, models, and experimental phenomena provide evidence of the existence of shallow bands in silicon induced by the dislocation strain field. Nevertheless, only deep bands, likely associated with contamination at dislocations, have been detected up to now by junction spectroscopy. Here we present the first experimental result by junction spectroscopy that assesses the existence of the dislocation related shallow states. These are found to be located at 70 and 60 meV from the valence and conduction band edge, respectively.

DOI: 10.1103/PhysRevLett.95.076401

PACS numbers: 71.55.Cn, 72.20.Jv

Si is inefficient as a light source as band-to-band optical emissions are improbable and most of the excited *e-h* pairs recombine nonradiatively. Nevertheless, there is a strong demand for an optical emitter compatible with standard silicon-based ultra-large-scale integration technology. For this reason since 1990 many strategies, recently reviewed [1], have been employed to overcome these materials limitations and to obtain efficient light emission from Si. One of the most successful is based on the modification of free carrier properties by quantum confinement effects, firstly obtained by the use of porous Si [2], then by the controlled production of Si nanocrystals in a SiO<sub>2</sub> matrix [3]. Another approach, derived from the results obtained in high efficiency solar cells, is based on the suppression of nonradiative recombination centers using for the device fabrication high quality substrates and defect passivation procedures [4].

This approach has evidenced the need of a deeper knowledge of dislocation related gap states, with a particular emphasis to their efficiency as radiative or nonradiative recombination centers and on the effectiveness of carrier confinement at dislocation related shallow bands.

Notwithstanding, theoretical and experimental studies on dislocations in silicon date back to the early fifties [5]; many aspects related to electrical properties and gap states of dislocations are still far to be understood. Furthermore, the subject of dislocation related band-gap states is really intriguing: although many experimental analyses revealed deep states in dislocated Si, theoretical investigations have assessed that straight 60° dislocations have reconstructed cores and are not associated with any deep band [5]. Theory [6] predicts relatively shallow bands to be associated with the dissociated dislocation strain field: in more detail an empty one-dimensional band *De* and a full one *Dh* have been predicted to split off from the conduction band and valence band edge, respectively.

*De* and *Dh* bands, even if never directly observed, have been related to various physical phenomena: such as dependence of the EBIC (electron-beam-induced current) contrast at dislocations on temperature and injection

dose [7], microwave conductance, electric-dipole spin resonance, and photoluminescence (PL) [5]. Consistent values for the position of the edges of the one-dimensional bands have been obtained [8]:  $E_C - E_{De} = E_{Dh} - E_V = 70\text{--}80\text{ meV}$  with *Ec* and *Ev* conduction and valence band edge, respectively, and *E<sub>De</sub>* and *E<sub>Dh</sub>* shallow band edges, respectively.

This Letter reports on experimental investigations concerning the characteristics of shallow states related with *De* and *Dh* bands. To this aim a very regular array of parallel 60° dislocations, introduced in silicon by an *ad hoc* designed plastic deformation procedure, is analyzed. Dislocation related shallow levels have been detected in this system by junction spectroscopy, and associated to *De* and *Dh* bands. To our knowledge, this is the first direct experimental clear observation of these shallow states and of their characteristics.

**Czochralski grown, (100), B-doped ( $\rho = 17\text{--}23\ \Omega\text{ cm}$ ),** Si was used in this study. As-grown samples are labeled “W” from now on. Dislocated samples were prepared by scratching the surface along the [110] direction and bending around the [110] direction for 1h at 670 °C in argon. The dislocation systems consist of half hexagonal loops of a screw and two 60° segments. In order to obtain a regular array of parallel 60° segments these samples, after having chemically removed the scratch, were submitted to a second deformation procedure identical to the previous one, to allow the expansion of the dislocation loops without a further dislocation nucleation. X-ray (XR) topography warranted in this case the practical absence of threading segments. These samples are labeled “DD” from now on. The dislocated samples were then annealed at 800 °C for 24 h in argon. These are labeled “DDTT” from now on. A control sample, labeled “C,” scratched but not deformed, annealed together with DDTT, was also analyzed by deep level transient spectroscopy (DLTS). Further details on the deformation procedure and on the dislocation systems are reported in Ref. [9].

Electrical investigation by DLTS and minority carrier transient spectroscopy (MCTS) have been carried out on

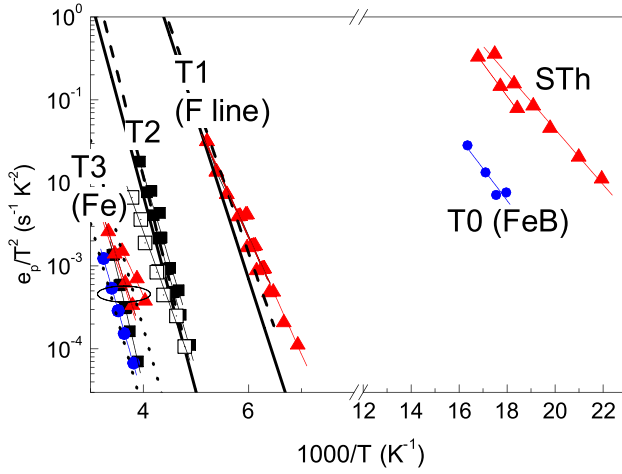


FIG. 1 (color online).  $T^2$ -corrected thermal emission rates as a function of inverse temperature for the DLTS lines  $T0$ ,  $T1$ ,  $T2$ ,  $T3$ , and  $STh$  found in  $W$  set (circle),  $DD$  set (square),  $DDTT$  (triangle). Thin solid lines represent data fitting. Literature data (thick lines) from Ref. [11] (solid lines), Ref. [12] (dashed lines), Ref. [13] (dotted lines), and Ref. [14] (open squares) are also reported.

these sample sets, previously studied by PL [9]. DLTS and MCTS [10] were performed by a SULA Tech. Inc. instrument, the sample temperature was varied from 20 to 350 K by means of a closed cycle helium cryostat (Cryophysics), the reverse bias from 6 to 0 V and the pulse width from 1 to

10 ms. MCTS was used to detect minority carrier (electron) traps. Above-band-gap light by a light-emitting device ( $\lambda = 650$  nm) provided the optical excitation of charge carriers while the sample was held under reverse bias. Semitransparent Schottky diodes were obtained on each sample by vacuum evaporation of Al. Current-voltage and capacitance-voltage characteristics were determined to test the diode ideality factors and the free carrier concentration, respectively.

DLTS analyses revealed the presence of several energy levels whose Arrhenius plots are reported in Fig. 1, while the trap characteristics are reported in Table I. Literature results relevant to hole traps detected in plastically deformed  $p$ -type Si [11,12] and to the well-known trap related to interstitial iron in Si [13] are also reported in Fig. 1.

First of all, three deep traps for holes ( $T3$ ,  $T2$ , and  $T1$ ) have been detected. Trap  $T3$  is made up by two different contributions (Table I): (i)  $T3a$ , which is present only in  $W$ ; (ii)  $T3b$ , present in plastically deformed samples ( $DD$  and  $DDTT$ ). These traps correspond to grown-in iron in different configuration:  $Fe_i$  in as-grown samples ( $W$ ), where the shallow trap  $T0$ , related to the FeB pair, is also detected (Table I) and the Fe-O complex in thermally treated samples ( $DD$ ,  $DDTT$ ), as reported also in Ref. [14].

The line  $T2$ , found only in  $DD$ , is in good agreement with the one of trap  $H(.49)$  of Ref. [12], corresponds to a broad and asymmetric peak in the DLTS spectra and is undetected in the annealed samples  $DDTT$ . The same line has been found also in oxygen precipitated Si [14] and in

TABLE I. Trap labels and characteristics.  $E_T$  activation enthalpy from the valence band edge for traps  $T3$ ,  $T2$ ,  $T1$ ,  $T0$ , and  $STh$ , from the conduction band edge for trap  $STe$ ;  $\sigma$  apparent capture cross section for holes ( $T3$ ,  $T2$ ,  $T1$ ,  $T0$ , and  $STh$ ) and electrons ( $STe$ );  $N_T$  trap concentration (only for DLTS analyses). All the trap concentrations have been evaluated in the samples with the highest dislocation density ( $10^7$  cm $^{-2}$ ).  $D4$  is the PL  $D4$  line [9].

Trap label $E_T$ (eV), $\sigma$ (cm $^2$ )		$N_T$ (cm $^3$ )			
		$W$	$DD$	$DDTT$	$C$
$T3$	$T3a$	$10^{12}$			
	0.44, $2 \times 10^{-17}$				
	$T3b$		$2 \times 10^{13}$	$1 \times 10^{13}$	$5 \times 10^{12}$
	0.36, $2 \times 10^{-18}$				
$T2$			$2 \times 10^{12}$		
	0.45, $2 \times 10^{-15}$				
$T1$				$7 \times 10^{12}$	
	0.28, $1.5 \times 10^{-16}$				
$T0$		$3 \times 10^{11}$			
	0.09, $2 \times 10^{-16}$				
$STh$				$10^{11}$	
	0.07, $10^{-15}$				
$STe$				$\checkmark$	
	0.06, $10^{-14}$				
$D4$			$\checkmark$		
	0.999				

plastically deformed Si [14] and attributed to point defect centers not localized at dislocations.

The line **T1**, found in *DDTT*, corresponds to the well-known *F* line (level *H.33* of Ref. [12], trap *T1* of Ref. [14]), found in plastically deformed Si and often related to impurities in the dislocation strain field [5].

Besides these deep traps two shallow traps for holes, labeled *T0* and *STh*, have been detected. The former, *T0*, with the same signature as the *FeB* pair [13], is detected only in as-grown samples (*W*), where *T3a* ( $\text{Fe}_i$ ) is also detected; thus it can be related to the *FeB* pair. The latter is a shallow hole trap (named *STh*), at  $E_v + 70$  meV, which appears only in *DDTT*, the plastically deformed and annealed samples. In these samples a shallow trap for minority carrier (electrons), labeled *STe*, has also been detected by MCTS (Table I). From now on we will mainly focus on the shallow traps *STh* and *STe*.

As iron is ubiquitously present in these samples, to a first guess *STh* and *T0* could both be related to the *FeB* pair that in Si introduces a level located around 0.1 eV from the valence band edge [13]. To check this hypothesis a photodissociation experiment [15] was carried out: the *DDTT* samples were lighted for 2 hours by focusing a 150 W quartz-tungsten-halogen (QTH) lamp on a 1 cm-diameter spot on the sample surface and analyzed by DLTS before and immediately after lighting. If this trap were related to *FeB* pairs, the photon energy would dissociate the pairs causing a reduction (or even the disappearance) of the *STh* peak and, correspondingly, an increase of the interstitial

iron related peak [13]. A similar experiment was carried out by heating the sample at 100 °C in vacuum for 1 h: but the DLTS spectra obtained before and after lighting (Fig. 2) and before and after heating are almost unchanged. These findings do demonstrate that *STh* is not related to the iron-boron pairs. The *FeB* pair is never detected in these samples likely due to the formation of a complex of Fe with O [14]: the cooling rate of the deformed samples is lower than that of the as-grown ones so that complex formation can occur; thus neither  $\text{Fe}_i$  neither *FeB* can be detected.

The capture kinetics of *STh* was studied by DLTS: the relevant spectra obtained at different filling pulse durations  $t_p$  (Fig. 3) show that the normalized maximum and the high *T* side of this peak keep constant (Fig. 3, inset) while the low-*T* side varies with  $t_p$ . Moreover, from the DLTS peak amplitude measured as a function of  $t_p$ , the trap density  $n_T$  versus  $t_p$  was obtained:  $n_T$  shows a logarithmic dependence on  $t_p$  (Fig. 4). These experimental findings are the signature of localized states at extended defects [16]. The logarithmic capture filling behavior reflects the presence of a repulsive potential  $\varphi(t)$  whose diagram is also reported in Fig. 4. The defect center becomes repulsive for holes when filled with holes, or in other words, when empty of electrons.

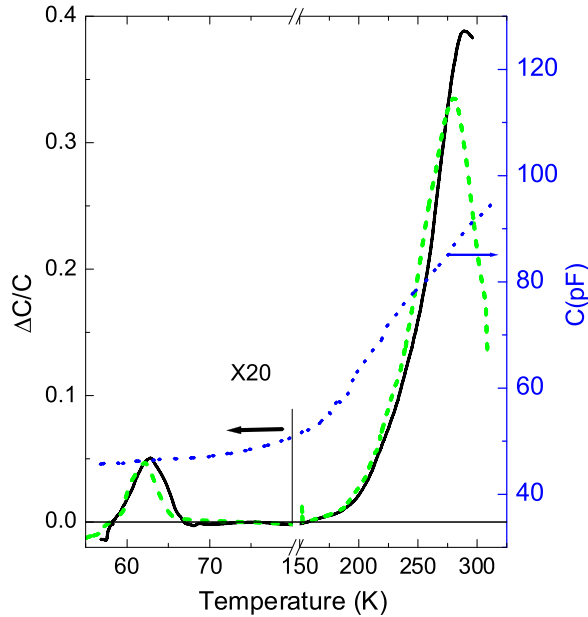


FIG. 2 (color online). DLTS spectra of a sample of the *DDTT* set before (solid line) and after (dashed line) lighting. Reverse bias  $-1.5$ , filling bias  $0$  V, filling pulse width  $10$  ms, rate window  $232.6 \text{ s}^{-1}$ . Lines *T1* and *T3* are convolved in one peak at this rate window. The  $C(T)$  curve is also reported (dotted line).

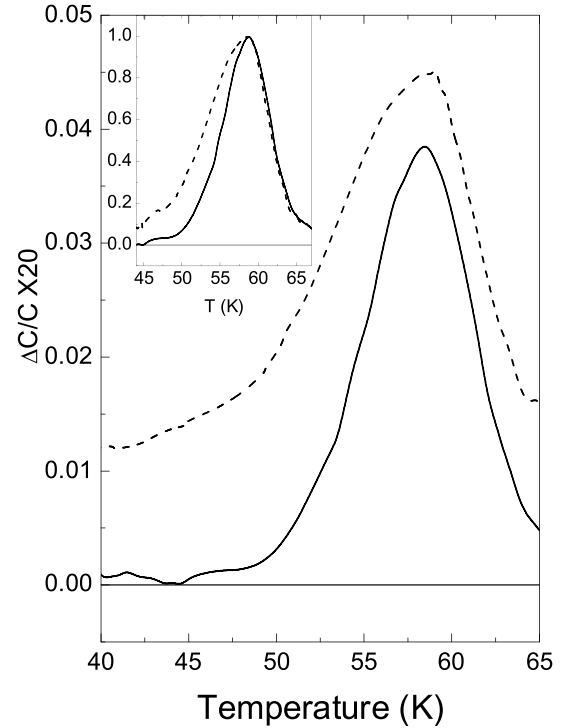


FIG. 3. DLTS spectra of *STh* trap measured at filling pulse width  $t_p = 1$  ms (solid line) and  $10$  ms (dashed line). Reverse bias  $-1.5$ , filling bias  $0$  V, rate window  $465.1 \text{ s}^{-1}$ . In the inset the signals normalized to the peak amplitudes are reported.

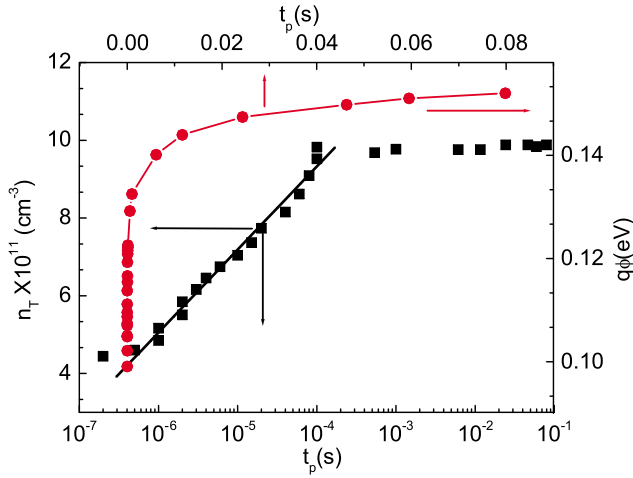


FIG. 4 (color online). STh trap concentration  $n_T$  as a function of the filling pulse width  $t_p$  (squares) and Coulomb barrier height evaluated vs  $t_p$  (circles). The hole capture cross section of STh, as measured by direct filling experiment, is equal to  $1.1 \times 10^{-16} \text{ cm}^2$ . The solid line is the linear fit of  $n_T$  vs  $\log(t_p)$ , the dotted line is only a guide for the eye.

In order to explore also minority carrier traps, MCTS analyses were carried out in *DDTT* samples. Besides a broad spectrum, a shallow trap for electrons (STe) located at around 0.06 eV from the conduction band edge, with apparent cross section of  $10^{-14} \text{ cm}^2$ , was observed (Table I).

In conclusion, the following results were obtained on the shallow levels STh and STe: (i) two shallow levels STe (for electrons) and STh (for holes) were detected by junction spectroscopy only in *DDTT* samples, where the deformation procedure was *ad hoc* designed in order to obtain a system of straight, nonintersecting  $60^\circ$  dislocations in absence of threading arms [9]. No evidence of STh was found in the *DD* set or in samples deformed with the standard procedure [14]; (ii) the photo-dissociation experiment excludes that STh would be related to the FeB centers; (iii) its capture kinetics shows that **STh is related to states localized at the extended defects ( $60^\circ$  dislocations)**; PL measurements carried out on the same sample sets [9] showed the canonical *D1*, *D2*, *D3*, and *D4* lines at 0.808, 0.843 and 0.945 and 0.99 eV in the *DD* samples (where the ***D4* emission is suggested to be related to transitions between *De* and *Dh* bands** [17,18]). On the contrary, only emissions associated to oxide nuclei (0.817 eV) and precipitates (0.830 and 0.850 eV) are collected from the *DDTT* samples. In these samples, the annealing treatment at  $800^\circ\text{C}$  after plastic deformation induces oxygen segregation at dislocations.

*De* and *Dh* shallow bands are predicted by theory to be located 0.07–0.08 eV below and above conduction and valence bands (CB, VB), respectively. In *DD* samples, which have clean  $60^\circ$  dislocations, free carrier capture

and emission from their band states to VB and CB would be too small to be detected by DLTS. Because of the annealing, the clean dislocations of *DD* set segregate O. Any variation in the structural properties of extended defects is accompanied by variations of its electronic properties, as reported in literature [19]; thus in *DDTT* set the dislocation related 1D shallow states have changed from bandlike to localized. Moreover, O segregation modifies both the electrostatic and elastic potentials at dislocations, increasing their electronic charge and, in turn, the charge carrier and capture emission probability in such a way that shallow states become detectable by DLTS in this set. In this respect, STh and STe can be considered related to the 1D bands *Dh* and *De*, respectively.

B. Pichaud (Lab. TECSN, Univ. Paul Cezanne, Aix-Marseille III) and S. Binetti (University of Milano-Bicocca) are gratefully acknowledged for sample preparation. This work was carried out in the frame of the DEDALES INTAS Contract No. 2000-0194.

- [1] L. Pavesi, J. Phys. Condens. Matter **15**, R1169 (2003).
- [2] L. T. Canham, Appl. Phys. Lett. **57**, 1046 (1990).
- [3] L. Pavesi, L. Dal Negro, C. Mazzoleni, G. Franzò, and F. Priolo, Nature (London) **408**, 440 (2000).
- [4] M. A. Green, J. Zhao, J. A. Wang, P. J. Reece, and M. Gal, Nature (London) **412**, 805 (2001).
- [5] W. Schröter and H. Cerva, in *Defect Interaction and Clustering*, edited by S. Pizzini (Trans Tech., Zürich, 2001), 1st ed., p. 67, and literature therein.
- [6] N. Lehto, Phys. Rev. B **55**, 15601 (1997).
- [7] V. Kveder, M. Kittler, and W. Schröter, Phys. Rev. B **63**, 115208 (2001).
- [8] V. Kveder, T. Sekiguchi, and K. Sumino, Phys. Rev. B **51**, 16721 (1995).
- [9] E. Leoni, S. Binetti, B. Pichaud, and S. Pizzini, Eur. Phys. J. Appl. Phys. **27**, 123 (2004).
- [10] J. A. Davidson and J. Evans, J. Appl. Phys. **81**, 251 (1997).
- [11] V. Kveder, Yu. Osipyan, W. Schroter, and G. Zoth, Phys. Status Solidi A **72**, 701 (1982).
- [12] C. Kisielowski and E. R. Weber, Phys. Rev. B **44**, 1600 (1991).
- [13] A. Istratov, H. Hieslmair, and E. R. Weber, Appl. Phys., A **69**, 13 (1999).
- [14] A. Castaldini, D. Cavalcoli, A. Cavallini, S. Binetti, and S. Pizzini, Appl. Phys. Lett. **86**, 162109 (2005).
- [15] J. Lagowski, P. Edelman, A. M. Kontkiewicz, O. Milic, W. Heley, M. Dexter, L. Jastrzebski, and A. M. Hoff, Appl. Phys. Lett. **63**, 3043 (1993).
- [16] W. Schroter, J. Kronewitz, U. Gnauert, F. Riedel, and M. Seibt, Phys. Rev. B **52**, 13726 (1995).
- [17] V. Higgs, F. Chin, X. Wang, J. Mosalski, and R. Beanland, J. Phys. Condens. Matter **12**, 10105 (2000).
- [18] V. Kveder, E. Steinman, S. Shevchenko, and H. Grimmeiss, Phys. Rev. B **51**, 10520 (1995).
- [19] F. Riedel and W. Schroeter, Phys. Rev. B **62**, 7150 (2000).